Anti-Cancer Activity of Titanium-Copper Alloy Coated with Silver Nanoparticles on Reduced Graphene Oxide Against Oral Squamous Carcinoma Cells

Mayada Faisel Khalil[1], Farah Tariq Muhammad Noori[2] and Sabah Anwer Salman[3]
[1]*Technical Institute of Baqubah, Middle Technical University, 32001 Baqubah, Iraq*
[2]*Department of Physics, College of Science, University of Baghdad, 10071 Baghdad, Iraq*
[3]*Department of Physics, College of Science, University of Diyala, 32001 Baqubah, Iraq*
mayada.faisel@gmail.com, farah_t258@yahoo.com, pro.dr_sabahanwer@yahoo.com

Keywords: Ti-Cu Alloy, Metallurgy, PLD, Hummer's Method, Reduced Graphene Oxide, Oral Squamous Carcinoma Cell Line.

Abstract: Ti alloys are frequently utilized in fields that have a significant impact like medicine, chemistry, and physics because of their exceptional properties. The properties of titanium alloys are affected by their composition and microstructure. This investigation intended to investigate the effects of different concentrations of copper 0, 0.5, 2.5, and 5 wt% on the cancerous cell line of the mouth coated with and without silver nanoparticles-Reduced graphene oxide (AgNps- rGO) sheets using Plus laser technology. The morphology and structural properties of the titanium-copper alloys were evaluated using scanning electron microscopy (SEM) and X-ray diffraction (XRD). The result show the weight percentage of copper and the coating layer of coated alloys were studied, 54% of the *Oral squamous cell carcinoma cell line (OSCC)* was killed by the (Ti-0%Cu) coated alloy, while 79% of the OSCC cell line was killed by the (Ti-5%Cu) coated alloy.The XRD results of the alloy before and after coating showed that the diffraction peaks are for the α-Ti phase, as well as slight peaks for the metallic Ti_2Cu phase, but no β-Ti peaks could be found. The (SEM) of the alloys prior to coating revealed that the pure titanium is uniformly dispersed throughout but the SEM images of the coated alloys revealed that the silver nanoparticles were distributed in a range of 20-26 nm with graphene oxide in a range of less than 100 nm.

1 INTRODUCTION

Tiny quantities are used as coatings or additives in nano-composite bio-applications in the contemporary period of material science research. In addition to being tiny or at the nanoscale, the nanomaterial offers rapid, inexpensive control over the structure of matter with a range of forms and morphologies since they are crucial elements in defining their qualities [1], [2]. These days, orthodontics, prosthodontics, and orthopedic surgical treatments employ a variety of metal materials, including porcelain, metal crowns, implants, mini-implants, brackets, archwires, screws, and plates. In certain procedures, nanoparticles of Ag, GO, Cu, and Au are created as antibacterial agents [3]. Titanium (Ti) compounds have become common in the dental industry because of their practical application [4], [5]. Applications include scenarios that call for smaller implants, high-stress locales, or thorough defect remedies [6]. These specifications need higher-quality materials, which are often achieved by adding chemical components to titanium. Implants may also have mechanical or biological problems [7]. Copper is important to the development of blood, nerve, and bone systems, as well as the proper maturation of these systems. Because of the copper's significant role in the human body, the number of scientists who seek to utilize its properties in the creation of new biomedical materials that benefit human health is increasing [8]-[10]. Increasing numbers of studies have demonstrated that biomaterials containing copper have a remarkable capacity [11], [12]. to preserve the cardiovascular system, shield themselves from bacteria, and promote healing of fractures [13]-[15]. Reduced graphene can be effectively used as a physical substrate in the design of tissues, as a means to transport drugs, cameras, and cancer therapies [16], [17]. In this study, graphene oxide was produced from green eucalyptus leaves using the Hummers method. Reduced graphene oxide nanoparticles (rGONPs) and silver nanoparticles (Ag NPs) were incorporated into a titanium-copper substrate by means of direct writing with a pulsed laser Deposition (PLD). This mixture was covered with a mixture that was employed as a cancer inhibitor for the oral cancer cell lines (OSCC). This research aims to fabricate Ti-Cu alloys with different copper concentrations and coat them with AgNPs-rGO nanoflakes to improve the structural, morphological and Anticancer Activity properties and study the effect of coating on inhibiting the growth and viability of oral squamous cell carcinoma cells.

2 MATERIALS AND METHODS

2.1 Materials

Natural graphite rod, $KMnO_2$ 99%, $NaNO_3$ 99.5%, H_2O_2 32%, HCl 37.5%, H_2SO_4 98% (from LOBA Chemie), NaOH 99% (from Dae-Jung), titanium 98% (from Fluka Chemika), copper 99.5% (from Chem-Lab), and eucalyptus leaves.

2.2 Synthesis and Reduction of Graphene Oxide

The most practical method of producing graphene oxide is the Hummer process. 1 gram of graphite is incorporated into the mixture of sulfuric acid and sodium nitrate in an ice bath for 45 minutes. Next, 3 g of potassium oxido manganese ($KMnO_2$) are added at a temperature of 35°C. The thick mixture is agitated for a day. The concentration of KMnO is decreased by adding 32% H_2O_2. The thick mixture is mixed with 5 ml of HCl 37.5% and deionized water. The mixture is heated to 75 °C for 5 hours in order to produce graphene oxide. The concentration of graphene oxide is decreased using eucalyptus leaves. After baking the leaves to temperatures of 100 °C, the product is then passed through a filter. After adding 1 mg of GO to 80 ml of eucalyptus fluid, the mixture is sonicated for 2 hours. The mixture is then placed on a magnetic stirrer and stirred at 45 °C for 12 hours. Ultimately, after passing through 80 °C filter paper, the product is placed in a temperature-controlled oven for 3 hours in order to dry [18].

2.3 Preparation Ti - Cu Alloy by Metallurgy Method

The substance was printed using a 600Map press. The cast iron had a diameter of 1.5 cm and a thickness of 1 mm, and was then heated in a furnace at 1250 °C for two hours.

2.4 Coating of Ti - Cu Alloy by Nanoparticles

The intended material is composed of 0.12 g of silver nanoparticles plus 1.2 g of graphene oxide that has been reduced with eucalyptus oil. After the pressure is applied, the target's diameter is 0.5 cm and its thickness is 1 mm. The framework of Nd-YA.G laser device, type HUA, FEI offering intermittent surges of 10.64nm (Q-switched) wave-length with energy per pulse of 400 mJ, number of pulses 200 pluses, repetition rate of 1Hz, with a convex lens of 100 mm to produce greater laser flounce, focal length must be increased.

2.5 Cytotoxicity Assays

The toxic effects of Ti-Cu alloys were determined using the MTT method in 6-well plates [19], [20]. Cell lines were grown at a concentration of 2 million cells per square meter. After 24 hours or after the cells formed a solid layer, the cells were tested for different concentrations of the substances in question. To determine the potency of the cells, the culture medium was removed after 72 hours of treatment, 500 µl of 2 mg/ml MTT solution was added to the wells, and the cells were incubated at 37 degrees Celsius for 2.5 hours. After the MTT washout, 500 µl of DMSO (Dimethyl sulfoxide) was added to the wells to dissociate any remaining crystals [21]. The mixture was then stirred and incubated at 37 °C for 15 minutes. The experiment was repeated three times, and the absorbance at 492 nm was measured using a microplate reader. The percentage of cytotoxicity was calculated according to the standard inhibition rate method described in previous studies [22], [23], based on the difference between the absorbance values of the control and treated samples.

The contrast of the control group's eyes is greater than the contrast of the sample group's eyes. After being coated with the virus, cells were cultured in

6-well microtiter plates at a concentration of 2×10^6 cells/ml and were incubated at 37 °C for 24 hours in the presence of a microscope [24]. Ti-(0, 0.5, 2.5, 5) % Cu was then added to the cells. After the exposure period, the plates were coated with crystal violet and incubated at 37 °C for 10 to 15 minutes. The dye was removed with water from the tap until all of the color was removed. The cells were observed at a 100x distance using an inverted microscope, images were then captured using a digital camera that was connected to the microscope.

2.5 Organism

The efficacy of the generated nanoparticles against cancer was determined using a cell type (OSCC). The human oral cancer cell lines were cultured in RPMI-1640 medium that contained 10% fetal bovine serum, 100 units of penicillin, and 100 µg of streptomycin. Cells were cultured with trypsin-EDTA and replated at a frequency of two weeks at a starting point of 80% confluence, the temperature of the cell culture was maintained at 37 °C [25], [26].

3 RESULTS AND DISCUSSION

3.1 Structural Properties of Titanium – Copper Alloy Coating by (AgNPs – rGO Nano Sheets)

Figure 1a shows the patterns of diffraction of the α-Ti phase and the weak peaks of the compound intermetallic Ti_2Cu, but no β-Ti peaks are present. Additionally, the intensity of the diffraction peak associated with the Ti-Cu alloy increases as the amount of Cu increases, this is indicative of a greater number of Ti-Cu precipitates [27], [28]. However, only one peak associated with theα-Ti phase was observed in Cu (0.5%), and the small volume fraction of the Ti2Cu phase was not observed by X-ray analysis of Cu. Additionally, the atomic diameters of the alloying and matrix components are less than 5% different, which is why it's typically believed that diffusion occurs between them. Since the atomic diameter of Ti is 13% greater than that of Cu, a migration between the two elements is observed. Because of the slow propagation of Ti and Cu atoms as a result of the heat treatment's slow cooling, a microstructure that is comprised of precipitated Ti_2Cu and the α-Ti phase is formed in the Ti-Cu alloy. However, since the rate of diffusion of Cu is greater than that of Ti in the presence of a thermal energy of activation, some of the Cu atoms can migrate into the Ti matrix and combine with the α-Ti [29]. As such, increasing the concentration of Cu by 2.5% can lead to the formation of α-Ti. Ultimately, the migration of Cu atoms and their response have an effect on the distribution and shape of the microstructure [30]. The results of the XRD study, the Ti-Ag phase diagram (not shown here) and the Ti-X%Cu composition in Figure 1b all show that Ag is primarily located in the matrix of titanium, rather than in any of the Ti-X phases, and these phases are not observed by XRD. due to the low content [31], [32].

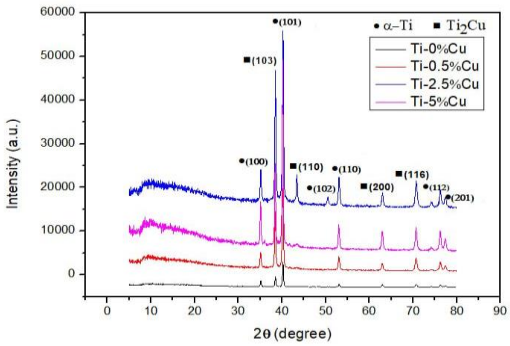

(a)

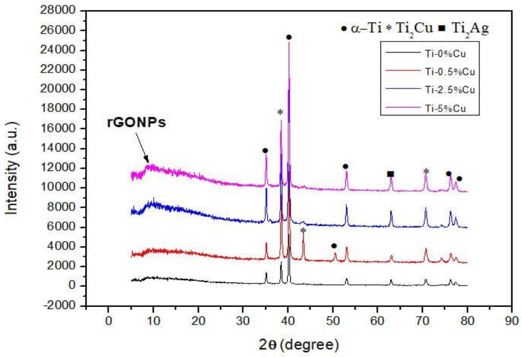

(b)

Figure 1: XRD patterns of Ti–X%Cu alloys: a) Ti–X%Cu alloys and b) Ti–X%Cu/AgNPs-rGONPs composite alloys.

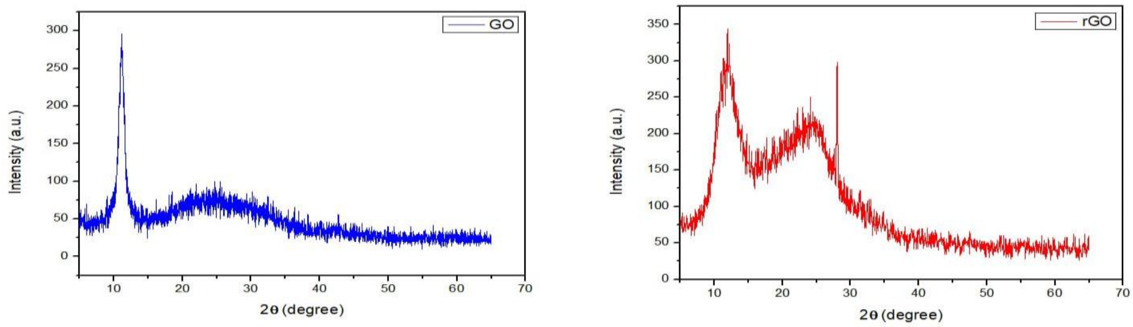

(a)

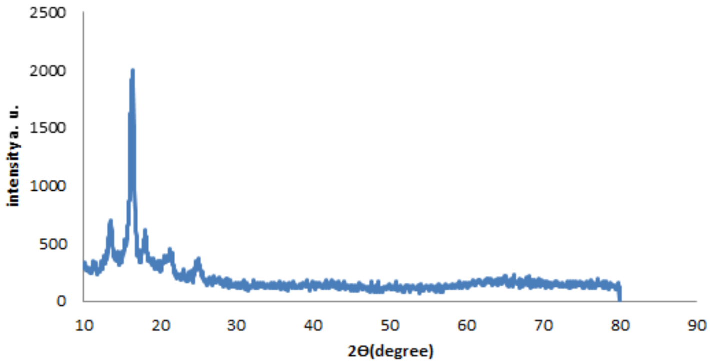

(b)

Figure 2: XRD analysis of graphene-based materials and AgNPs-rGO nanocomposite: a) XRD patterns of graphene oxide (GO) and reduced graphene oxide (rGO), and b) XRD pattern of AgNPs-rGO coating.

Figure 2a shows the patterns of X-ray diffraction that are associated with GO and rGO. The method of creating graphene oxide is said to be effective, the peak is at ($2\theta = 11.22°$) and the d-spacing is (7.87 Å). Increasing the d-spacing of graphite (d = 4.35 Å) causes this chemical process to increase, as the generated functional groups of oxygen form carboxyl, hydroxyl, and epoxy between the layers of graphite. Reduced graphene (rGO) facilitates the removal of functional groups based on oxygen, it has a maximum at ($2\theta = 26.2°$) and a d-spacing of 4.87 Å. While both GO and rGO are hexagonal, the AgNPs-rGO coating in Figure 2b has a hexagonal structure. The presence of AgNPs in a crystalline form is demonstrated by the five distinct diffraction patterns (2θ = 12.37, 13.67, 16.32, 18.12, 21.52, 24.87) ° from the planes ((100), (111), (200), (220) (311)) of the face-centered cubic (FCC) crystal structure.

3.2 Morphology Properties of Titanium - Copper Alloy Coating by (AgNPs-rGO) Nano Sheet

To investigate the evolution of microstructure and recognize the phases, two different microstructures of Ti-Cu were observed SEM. Figure 3a shows SEM images of Ti-0%Cu, Ti-0.5%Cu, Ti-2.5%Cu, and Ti-5%Cu, which were derived from the corresponding EDS investigations. In the SEM images of the Ti-0%Cu sample, all of the titanium is located in the middle. Meanwhile, small, dissociated precipitation particles with a width of 200-800nm appeared in the matrix of the Ti-0.5%Cu, Ti-2.5%Cu, and Ti-5%Cu alloys, these were recognized as being of the Ti-Cu type by EDS analysis.

Also, the thin, rectangular-shaped phases in the SEM images are separated by organized, spherical particles called Ti-Cu [33]-[35]. Figure 3b shows images of the SEM type Ti-0%Cu, Ti-0.5%Cu, Ti-2.5%Cu, and Ti-5%Cu, as well as their corresponding EDS analysis using a target that is composed of PLD material (AgNPs-rGO sheets). The SEM images indicate that the AgNPs are spread out around 20-26nm, while the rGO sheets are distributed around 100nm. Figure 4a shows an EDS image of a Ti-Cu alloy that was produced using a metallurgical method, while Figure 4b shows an EDS image of a Ti-Cu alloy that was produced using an AgNPs-rGO coating that is intended for use in healthcare.

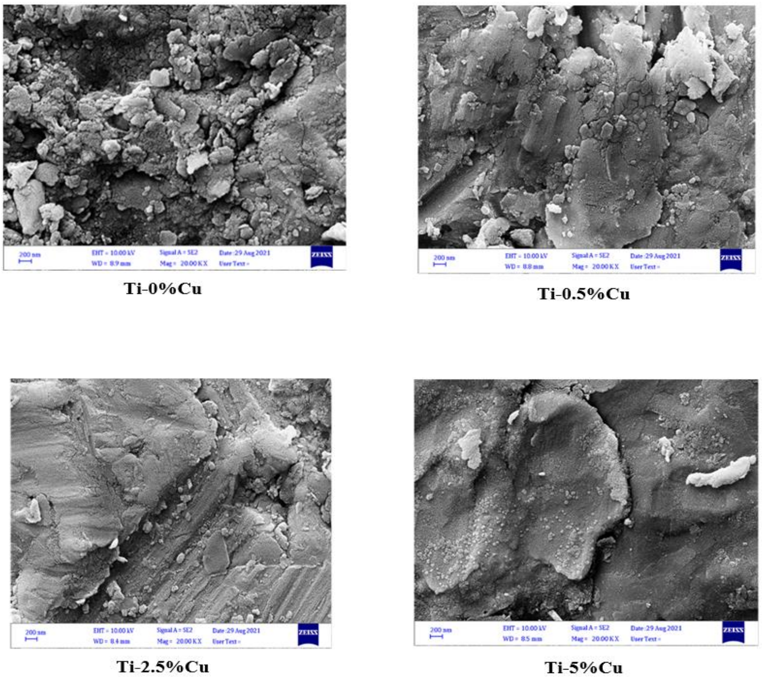

(a)

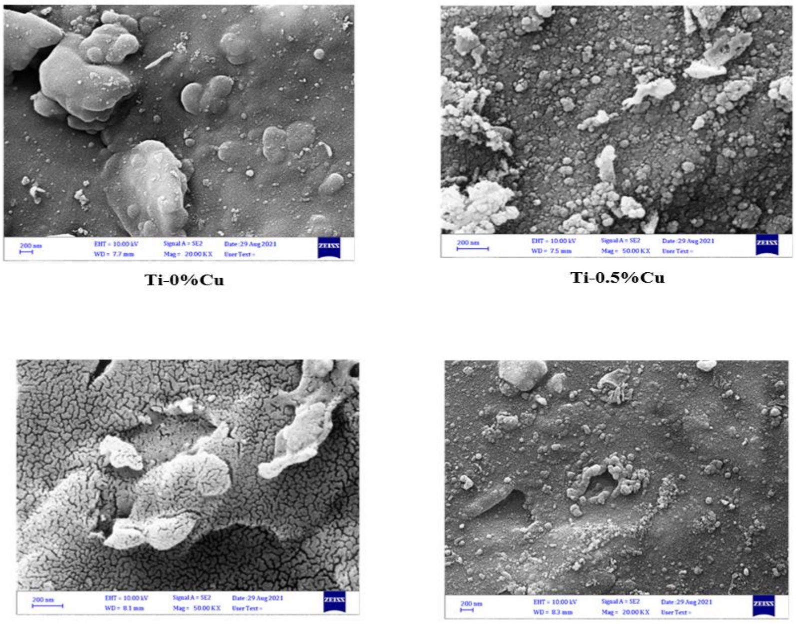

(b)

Figure 3: SEM micrographs of the prepared Ti–X%Cu alloys: a) uncoated Ti–X%Cu alloys and b) Ti–X%Cu alloys coated with AgNPs-rGONPs.

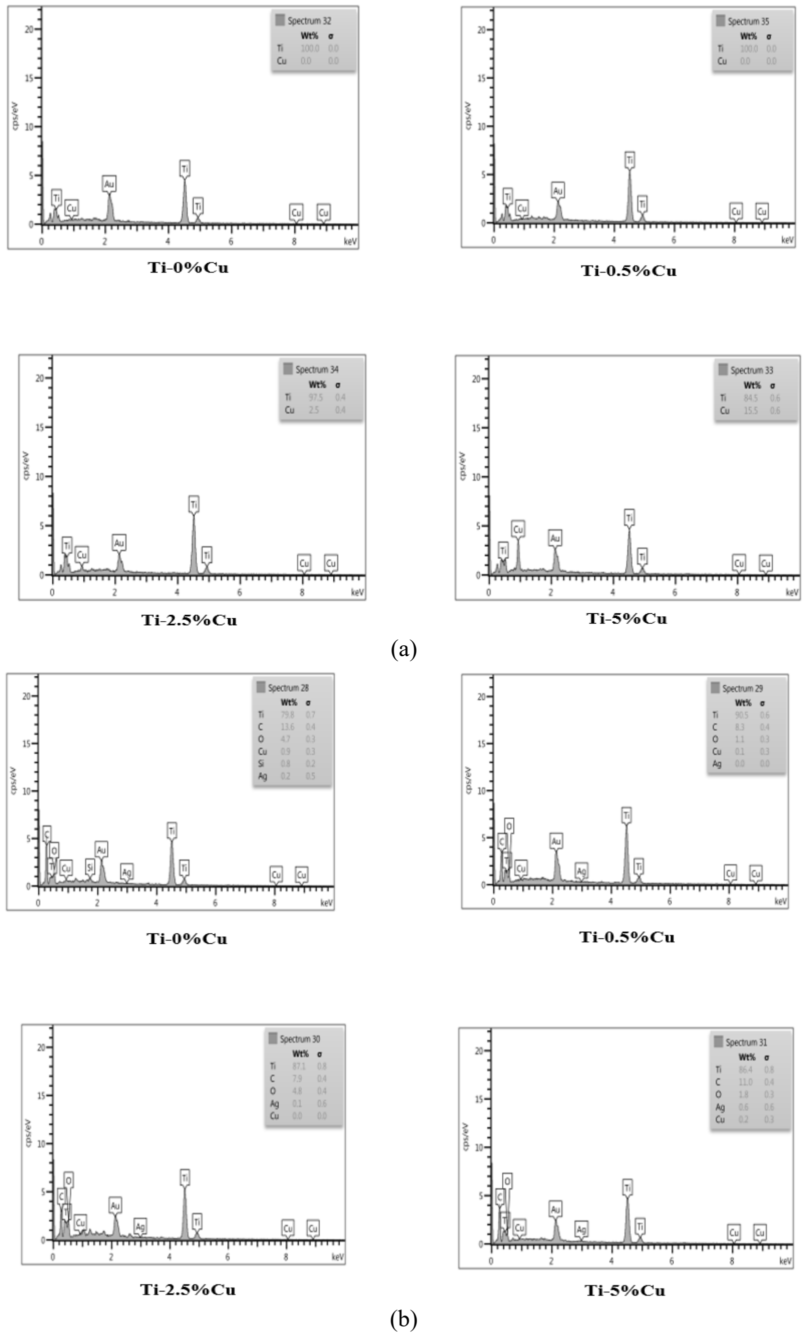

Figure 4: EDS spectra of the prepared Ti–X%Cu alloys: a) uncoated Ti–X%Cu alloys and b) Ti–X%Cu alloys coated with AgNPs-rGONPs.

4.3 Anticancer Activity

The toxic effects of Ti-0, 0.5, 2.5 and 5 wt% Cu on orally derived squamous cell carcinoma cells were studied. The effectiveness of the anti-cancer agent Ti-0, 0.5, 2.5 and 5 wt% Cu was determined by its capacity to inhibit the proliferation of cancer cells. The results of (Ti-0%Cu) alloy destroyed 54% of OSCC cells, whereas a (Ti-5%Cu) alloy killed 79% of OSCC cells, as demonstrated in Figure 5. Morphology alterations in OSCC cell lines were also analyzed for evidence of apoptosis. The morphology of the treated cells was similar to that of the control cells. When treated with (Ti-Cu) coated alloys containing varying concentrations of Cu, nevertheless, OSCC cell lines displayed morphological changes. There was a considerable reduction in the number of OSCC cell colonies in the presence of AgNPs-rGONPs-treated (Ti-Cu) coated alloys [36], as demonstrated in Figure 6.

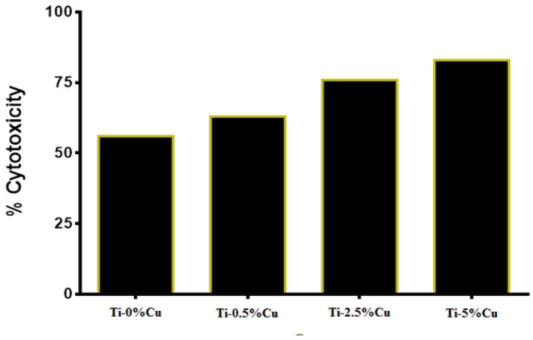

Figure 5: Cytotoxic effect of Ti-(0, 0.5, 2.5, 5) % Cu in OSCC cells.

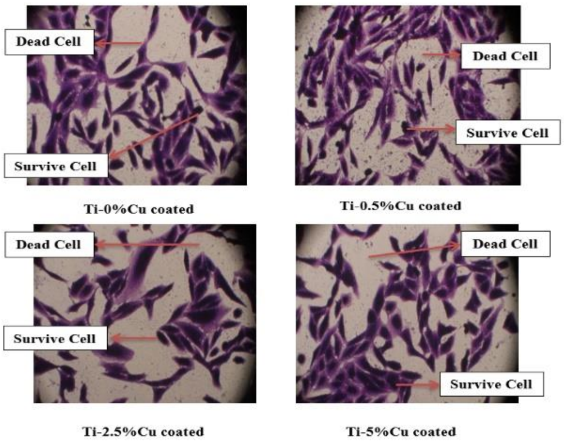

Figure 6. Morphological changes in OSCC cells after PLD for (Ti- 0,0.5, 2.5, 5)% Cu. (M.p. power).

4 CONCLUSIONS

This research demonstrates that the coating of Ti-0, 0.5, 2.5 and 5 wt% Cu alloys with a dose- and time-dependent effect on the toxicity of the cells of the oral cavity shows that these compounds have a significant effect on the cells of the oral cavity in comparison to existing therapeutic agents that have a similar cost, but are less toxic, and have fewer side effects. Additionally, a dual-phase Ti2Cu was created via a preplanning metallurgical approach using α-Ti. Covered Ti-0, 0.5, 2.5 and 5 wt% Cu alloys (Ag NPs-rGO sheets) had a superior compatibility with biological systems than uncovered Ti-0, 0.5, 2.5 and 5 wt% Cu, and the study conclusively demonstrated that the copper-bearing titanium alloy (Ti-Cu) possesses potent anti-cancer properties against oral squamous cell carcinoma (OSCC). A clear increase in the cytotoxic effectiveness against cancer cells was observed with increasing copper concentration. Specifically, the (Ti-5%Cu) alloy resulted in the destruction of 79% of the OSCC cells, representing a significant superiority when compared to the control alloy, (Ti-0%Cu), which destroyed 54% of the cells. Furthermore, analysis of the treated cells confirmed that the (Ti-Cu) alloys, across varying copper concentrations, induce distinct morphological changes in OSCC cell lines. These changes are indicative of the activation of the apoptotic pathway (programmed cell death). Overall, these findings establish that the incorporation of copper into titanium alloys is a successful strategy for creating implant materials with active therapeutic properties against oral cancer cells.

ACKNOWLEDGMENTS

The authors would like to express their sincere gratitude to the Department of Physics, College of Science, University of Diyala, and University of Baghdad for their assistance provision of the necessary facilities to conduct this research.

REFERENCES

[1] S. Panhwar, et al., “Importance and analytical perspective of green synthetic strategies of copper, zinc, and titanium oxide nanoparticles and their applications in pathogens and environmental remediation,” Current Anal. Chem., vol. 17, pp. 1-17, 2021, [Online]. Available: https://doi.org/10.2174/15734110169992005291410 11.

[2] F. T. M. Noori, A. Kadhim, and N. D. Hamza, “Optical and structural properties of ZnO:Au nanocomposite thin films,” Int. J. Nanoelectron. Mater., vol. 11, pp. 347-356, 2018, [Online]. Available: https://doi.org/10.33923/ijonem.2018.11.03.347-356.

[3] B. Bai, E. Zhang, J. Liu, and J. Zhu, “The anti-bacterial activity of titanium-copper sintered alloy against Porphyromonas gingivalis in vitro,” Dent. Mater. J., vol. 35, no. 4, pp. 659-667, 2016, [Online]. Available: https://doi.org/10.4012/dmj.2016-001.

[4] M. Geetha, A. K. Singh, R. Asokamani, and A. K. Gogia, “Ti based biomaterials: the ultimate choice for orthopaedic implants – a review,” Prog. Mater. Sci., vol. 54, pp. 397-425, 2009, [Online]. Available: https://doi.org/10.1016/j.pmatsci.2008.06.004.

[5] F. T. Noori and M. K. Khalaf, “Corrosion resistance of Ti6Al4V alloy by radio frequency technique used for coating deposition of multilayer (HA/TiN/Ti6Al4V-substrate) for optimization power,” in IOP Conf. Ser.: Mater. Sci. Eng., vol. 757, p. 012047, 2020, [Online]. Available: https://doi.org/10.1088/1757-899X/757/1/012047.

[6] H. M. Grandin, S. Berner, and M. Dard, “A review of titanium-zirconium (TiZr) alloys for use in endosseous dental implants,” Materials (Basel), vol. 5, pp. 1348-1360, 2012, [Online]. Available: https://doi.org/10.3390/ma5081348.

[7] P. Stenlund, O. Omar, U. Brohede, S. Norgren, B. Norlindh, A. Johansson, J. Lausmaa, P. Thomsen, and A. Palmquist, “Bone response to a novel Ti–Ta–Nb–Zr alloy,” Acta Biomater., vol. 20, pp. 165-175, 2015, [Online]. Available: https://doi.org/10.1016/j.actbio.2015.03.038.

[8] L. Ren, H. M. Wong, C. H. Yan, K. W. K. Yeung, and K. Yang, “Osteogenic ability of Cu-bearing stainless steel,” J. Biomed. Mater. Res. B Appl. Biomater., vol. 103, pp. 1433-1444, 2015, [Online]. Available: https://doi.org/10.1002/jbm.b.33314.

[9] Y. Zhuang, S. Zhang, K. Yang, L. Ren, and K. Dai, “Antibacterial activity of copper-bearing 316L stainless steel for the prevention of implant-related infection,” J. Biomed. Mater. Res. B Appl. Biomater., vol. 108, pp. 484-495, 2020, [Online]. Available: https://doi.org/10.1002/jbm.b.34407.

[10] E. L. Zhang, et al., “Role of Cu element in biomedical metal alloy design,” Rare Met., vol. 38, pp. 476-494, 2019, [Online]. Available: https://doi.org/10.1007/s12598-019-01200-2.

[11] Q. Huang, Z. Ouyang, Y. Tan, H. Wu, and Y. Liu, “Activating macrophages for enhanced osteogenic and bactericidal performance by Cu ion release from micro/nano-topographical coating on a titanium substrate,” Acta Biomater., vol. 100, pp. 415-426, 2019, [Online]. Available: https://doi.org/10.1016/j.actbio.2019.09.030.

[12] R. Liu, Z. Ma, S. K. Kolawole, L. Zeng, Y. Zhao, L. Ren, and K. Yang, “In vitro study on cytocompatibility and osteogenesis ability of Ti-Cu alloy,” J. Mater. Sci. Mater. Med., vol. 30, p. 75, 2019, [Online]. Available: https://doi.org/10.1007/s10856-019-6277-z.

[13] V. Georgakilas et al., “Functionalization of Graphene: Covalent and Non-Covalent Approaches, Derivatives and Applications,” Chem. Rev., vol. 112, no. 11, pp. 6156-6214, Nov. 2012, [Online]. Available: https://doi.org/10.1021/cr3000412.

[14] M. Gu et al., “Is Graphene a Promising Nanomaterial for Promoting Surface Modification of Implants or Scaffold Materials in Bone Tissue Engineering?,” Tissue Eng. B Rev., vol. 20, no. 5, pp. 477-491, Oct. 2014, [Online]. Available: https://doi.org/10.1089/ten.teb.2014.0044.

[15] W. C. Lee et al., “Origin of Enhanced Stem Cell Growth and Differentiation on Graphene and Graphene Oxide,” ACS Nano, vol. 5, no. 9, pp. 7334-7341, Sep. 2011, [Online]. Available: https://doi.org/10.1021/nn202111e.

[16] W. Chen et al., “Composites of Aminodextran-Coated Fe3O4 Nanoparticles and Graphene Oxide for Cellular Magnetic Resonance Imaging,” ACS Appl. Mater. Interfaces, vol. 3, no. 10, pp. 4085-4091, Oct. 2011, [Online]. Available: https://doi.org/10.1021/am2008316.

[17] H. Wu et al., “Improvement of Photoluminescence of Graphene Quantum Dots with a Biocompatible Photochemical Reduction Pathway and its Bioimaging Application,” ACS Appl. Mater. Interfaces, vol. 5, no. 4, pp. 1174-1179, Feb. 2013, [Online]. Available: https://doi.org/10.1021/am302787c.

[18] H. A. Abdulmageed et al., “Green Synthesis of Reduced Graphene Oxide by Green Tea Leaves,” in J. Phys. Conf. Ser., vol. 1795, no. 1, p. 012070, Feb. 2021, [Online]. Available: https://doi.org/10.1088/1742-6596/1795/1/012070.

[19] H. N. K. Al-Salman et al., “2-Benzhydrylsulfinyl N-Hydroxyacetamide Na Extracted from Fig as a Novel Cytotoxic and Apoptosis Inducer in SKOV-3 and AMJ-13 Cell Lines via P53 and Caspase-8 Pathway,” Eur. Food Res. Technol., vol. 246, no. 8, pp. 1591-1608, Aug. 2020, [Online]. Available: https://doi.org/10.1007/s00217-020-03525-4.

[20] M. S. Jabir et al., “Supermagnetic Fe3O4-PEG Nanoparticles Combined with NIR Laser and Alternating Magnetic Field as Potent Anti-Cancer Agent Against Human Ovarian Cancer Cells,” Mater. Res. Express, vol. 6, no. 11, p. 115412, Nov. 2019, [Online]. Available: https://doi.org/10.1088/2053-1591/ab5204.

[21] A. G. Al-Ziaydi et al., “Newcastle Disease Virus Suppresses Glycolysis Pathway and Induces Breast Cancer Cell Death,” Bioengineering, vol. 31, no. 4, pp. 341-348, Apr. 2020, [Online]. Available: https://doi.org/10.1134/S0006359020040032.

[22] K. S. Khashan, M. S. Jabir, and F. A. Abdulameer, “Carbon Nanoparticles Prepared by Laser Ablation in Liquid Environment,” Surf. Rev. Lett., vol. 26, no. 06, p. 1950078, Jun. 2019, [Online]. Available: https://doi.org/10.1142/S0218625X19500782.

[23] S. H. Kareem et al., “Polyvinylpyrrolidone-Loaded MnZnFe2O4 Magnetic Nanocomposites Induce Apoptosis in Cancer Cells Through Mitochondrial Damage and P53 Pathway,” J. Inorg. Organomet. Polym. Mater., vol. 30, no. 13, pp. 5009-5023, Dec. 2020, [Online]. Available: https://doi.org/10.1007/s10904-020-01683-1.

[24] M. S. Jabir et al., “Green Synthesis of Silver Nanoparticles from Eriobotrya japonica Extract: A Promising Approach Against Cancer Cell Proliferation, Inflammation, Allergic Disorders and Phagocytosis Induction,” Artif. Cells Nanomed. Biotechnol., vol. 49, no. 1, pp. 48-60, Jan. 2021, [Online]. Available: https://doi.org/10.1080/21691401.2020.1856710.

[25] K. S. Khashan et al., “Synthesis, Characterization and Evaluation of Antibacterial, Anti-Parasitic and Anti-Cancer Activities of Aluminum-Doped Zinc Oxide Nanoparticles,” J. Inorg. Organomet. Polym. Mater., vol. 30, no. 13, pp. 3677-3693, Nov. 2020, [Online]. Available: https://doi.org/10.1007/s10904-020-01648-4.

[26] J. Majid et al., “Linalool-Loaded Glutathione-Modified Gold Nanoparticles Conjugated with CALNN Peptide as Apoptosis Inducer and NF-κB Translocation Inhibitor in SKOV-3 Cell Line,” Int. J. Nanomed., vol. 15, pp. 9025-9047, Nov. 2020, [Online]. Available: https://doi.org/10.2147/IJN.S280916.

[27] R. Liu et al., “In Vitro and In Vivo Studies of Anti-Bacterial Copper-Bearing Titanium Alloy for Dental Application,” Dental Mater., vol. 34, no. 8, pp. 1112-1126, Aug. 2018, [Online]. Available: https://doi.org/10.1016/j.dental.2018.05.013.

[28] S. L. Warnes and C. W. Keevil, “Mechanism of Copper Surface Toxicity in Vancomycin-Resistant Enterococci Following Wet or Dry Surface Contact,” Appl. Environ. Microbiol., vol. 77, no. 17, pp. 6049-6059, Sep. 2011, [Online]. Available: https://doi.org/10.1128/AEM.00401-11.

[29] C. C. Yi et al., “Antibacterial Ti-Cu Alloy with Enhanced Mechanical Properties for Implant Applications,” Mater. Res. Express, vol. 7, no. 10, p. 105404, Oct. 2020, [Online]. Available: https://doi.org/10.1088/2053-1591/abbae2.

[30] Z. Q. Chen, Y. G. Li, and M. H. Loretto, “Role of Alloying Elements in Microstructures of Beta Titanium Alloys with Carbon Additions,” J. Mater. Sci. Technol., vol. 19, no. 6, pp. 1391-1398, Nov. 2003, [Online]. Available: https://doi.org/10.1016/S1005-0302(01)70817-X.

[31] M. K. Kang et al., “Antibacterial Effect of Sand-Blasted, Large-Grit, Acid-Etched Treated Ti–Ag Alloys,” Mater. Res. Bull., vol. 47, no. 10, pp. 2952-2955, Oct. 2012, [Online]. Available: https://doi.org/10.1016/j.materresbull.2012.07.030.

[32] A. Shi et al., “What Controls the Antibacterial Activity of Ti-Ag Alloy, Ag Ion or Ti2Ag Particles,” Mater. Sci. Eng. C, vol. 109, p. 110688, Apr. 2022, [Online]. Available: https://doi.org/10.1016/j.msec.2019.110688.

[33] J. Liu et al., “The Antibacterial Properties and Biocompatibility of a Ti–Cu Sintered Alloy for Biomedical Application,” Biomed. Mater., vol. 9, no. 2, p. 025013, Apr. 2014, [Online]. Available: https://doi.org/10.1088/1748-6041/9/2/025013.

[34] J. O’Gorman and H. Humphreys, “Application of Copper to Prevent and Control Infection: Where Are We Now?,” J. Hosp. Infect., vol. 81, no. 4, pp. 217-223, Aug. 2012, [Online]. Available: https://doi.org/10.1016/j.jhin.2012.04.010.

[35] C. E. Santo et al., “Bacterial Killing by Dry Metallic Copper Surfaces,” Appl. Environ. Microbiol., vol. 77, no. 3, pp. 794-802, Feb. 2011, [Online]. Available: https://doi.org/10.1128/AEM.01934-10.

[36] J. Wang, “Optimization of Mechanical Property, Antibacterial Property and Corrosion Resistance of Ti-Cu Alloy for Dental Implant,” J. Mater. Sci. Technol., vol. 35, no. 11, pp. 2336-2344, Nov. 2019, [Online]. Available: https://doi.org/10.1016/j.jmst.2019.05.025.